# X-ray determination of atomic short-range order in the spin-glass system *Au*Fe

E. Dartyge, H. Bouchiat, and P. Monod
*Laboratoire de Physique des Solides, Université de Paris-Sud-91405 Orsay, France*
(Received 13 April 1981; revised manuscript received 13 July 1981).

Diffuse x-ray measurements carried out on *Au*Fe single crystals of 14.4, 15.4, and 19 at. % Fe show evidence for short-range order quite different in nature from that found in *Ag*Mn and *Cu*Mn alloys. This short-range order is seen as (1) a strong small-angle scatterings suggesting a tendency towards segregation, (2) a system of diffuse streaks extending in a discontinuous manner along $\langle 1\ \frac{1}{2}\ 0 \rangle$ axes and equivalents, and (3) an asymmetry of the diffuse streaks about each Bragg spot. We interpret this ensemble of facts by the existence of Fe-rich platelets oriented parallel to { 420 } planes, about two-planes thick and extending 30 Å parallel to their plane.

## I. INTRODUCTION

Since the early discovery[1] of what are now generally termed spin-glasses[2] the microscopic description of the organization of the spins in real space has long been a controversial question. The answer to this question has usually followed one of three approaches summarized below and also compared in Ref. 3. On one hand, the theoretical description of the spin-glass transition as a genuine phase transition implies a homogeneous order parameter (however complex it may be) which is zero above the spin-glass temperature $T_g$ and increases steadily below this temperature.[4] Since the mean-field hypothesis used is only valid for infinite-range interactions, this approach ignores the possiblity of "local" spin arrangements of a finite size and is therefore intrinsically insensitive to the existence of short-range order among the spins at least for the determination of the transition temperature. However, as we shall see, this result seems to be in surprising agreement with the small amount of existing data.

The two other analyses specifically involve the existence of some local order among the spins. The scaling-law analysis proposed by Souletie and Tournier[5] after the initial work of Blandin[6] makes use of the fact that the Ruderman-Kittel exchange among the spins scales with the inverse cube of the distance between them. Thus, all properties depending on the interaction energy should obey universal laws when scaled with the concentration for a completely random alloy. Such an analysis has been used successfully to find "universal" laws for thermodynamic quantities and also metastable properties (such as the remanent magnetization) for a large class of alloys. This line of reasoning has now been inverted in the sense that the existence of scaling properties can be considered as strong evidence for randomness among the spins. From a dimensional analysis involving the exchange interactions and an anisotropy energy (assumed to be dipolar), Tholence and Tournier[7] proposed further that the elementary "building blocks" of the spin-glass phase would consist of groups of spins whose sizes are adjusted to give the right order of magnitude for the remanent magnetization, by a statistical argument. In all cases only a few thousand spins are involved, independent of concentration. In this model, the existence of nonrandomness, i.e., short-range order on a scale comparable to these elementary "building blocks," should have a profound effect on all properties and should manifest itself clearly as strong deviations from the scaling laws.

The last type of analysis has been pursued by Beck and co-workers[8,9] and consists of fitting the properties of the magnetization at $T_g$ (and above it) to Curie-Weiss parameters from which the effective size of superparamagnetic clusters of spins, together with their mean interaction, is determined. According to Anderson,[3] the nonlinear behavior of the magnetization at low fields in this range of temperature is bound to yield unphysically large moments through the use of this method. However, the merit of Beck's approach is to point out experimentally the very sensitive nature of the magnetization in this region to various metallurgical treatments.

Within the framework of these models a number of workers have attempted to draw conclusions concerning the spatial coherence of groups of spins

 

in these alloys from measurements of different magnetic properties: susceptibility,[10–12] low-field magnetization,[8,9,11–14] high-field magnetization,[15] Mossbauer effects,[16] and neutron small-angle scattering.[17]

In contrast with this enormous amount of magnetic data, very little effort, if any, has been devoted to the actual determination of the atomic short-range order of these alloy systems by *direct* means, i.e., x-ray diffuse scattering or neutron diffraction and extended x-ray absorption fine-structure (EXAFS) measurements.[18]

A notable exception exists for the system *Cu*Mn, which has received detailed attention by Sato and co-workers,[19] following the early work of Meneghetti and Sidhu.[20] Recently we have performed a similar determination of short-range order on *Ag*Mn using x-ray techniques[21] (instead of neutrons necessary for the *Cu*Mn system). One of our conclusions was that the type of short-range order is very similar in both systems but does not correspond to that inferred by Sato *et al.*[19,21] It appears that no such determination has yet been carried out for the *Au*Fe system. Considering the importance of this alloy it is the purpose of this paper to present our results concerning the description and the analysis of the short range order in alloys of *Au*Fe in the concentration range 14%–19% and to compare these with those previously obtained on *Ag*Mn.[21]

## II. SAMPLES AND TECHNIQUES

As the x-ray technique used in our investigation required single-crystal samples we had to restrict the range of concentration of our study to that where the short-range order might be quite visible and play an important role in the magnetic properties. In view of our previous study of the *Ag*Mn system,[21] where we could gradually follow the appearance of short-range order from 6% Mn to 24% Mn, we chose to take three Fe concentrations in Au just spanning the spin-glass ferromagnetic transition.[10] These concentrations were determined by x-ray microprobe analysis[22] to be, respectively, 14.4, 15.4, and 19 at. % Fe. The single crystals were prepared by the Bridgman technique[23] by slowly moving the alloy (typically 48 h) through a temperature gradient. The ingot was held in a quartz tube under vacuum. The samples were quenched in water from temperatures near their melting point, then stored in liquid nitrogen. The sample with 14.4 at. % concentration was, however, slowly cooled in nitrogen atmosphere from 1000 to 650 °C and then quenched in water at room temperature, since it has been reported[10] that the quenching is more effective from 650 °C than for higher temperatures. No qualitative difference was observed, however, between the diffraction patterns of the crystals quenched from 1000 °C and from 650 °C. The resulting single crystal with a volume of about 1 $cm^3$ and grown along some random direction was then cut into $\sim 0.1$-mm slices (after preliminary orientation with a Laue photograph) and further etched in aqua regia down to a final thickness ($\sim 20$ $\mu$m) compatible with the x-ray transmission experiment. Two kinds of x-ray diffuse-scattering photographs were taken. The first kind of photograph involved use of a fixed film and a fixed sample in order to examine a large fraction of reciprocal space within a relatively short exposure time (12–24 h) at the cost of the increased complexity of analysis of such diagrams. The second type was by means of a Buerger-precession method[24] enabling one to select one plane in reciprocal space but with an inherently much longer exposure time (two weeks).

## III. *Au*Fe SHORT-RANGE ORDER

### A. Description of the diffuse x-ray patterns

Diffuse scattered intensity was observed on fixed crystal photographs for the 14.4%, 15.4%, and 19% alloys with little, if any, qualitative changes observed within this range of concentration. Figure 1 gives an example of what is obtained with the fixed crystal method. In addition to the Bragg spots (overexposed) and thermal diffuse scattering, one can see an array of diffuse streaks which links the Bragg spots to the $(1,\frac{1}{2},0,)$ and equivalent points of the cubic system. The half-width in a direction perpendicular to the diffuse streaks was estimated from microdensitometric measurements to be $\frac{1}{8}$ of a cubic reciprocal cell. The diffuse streaks are observed more readily at small values of the scattering vector and appear to decrease rapidly in intensity at larger angles. Their intensity, however, is enhanced at $(1,\frac{1}{2},0)$ and equivalent points in reciprocal space. Furthermore, one notices a strong isotropic-diffuse scattering at small angles.

The indexing of the patterns obtained for dif-

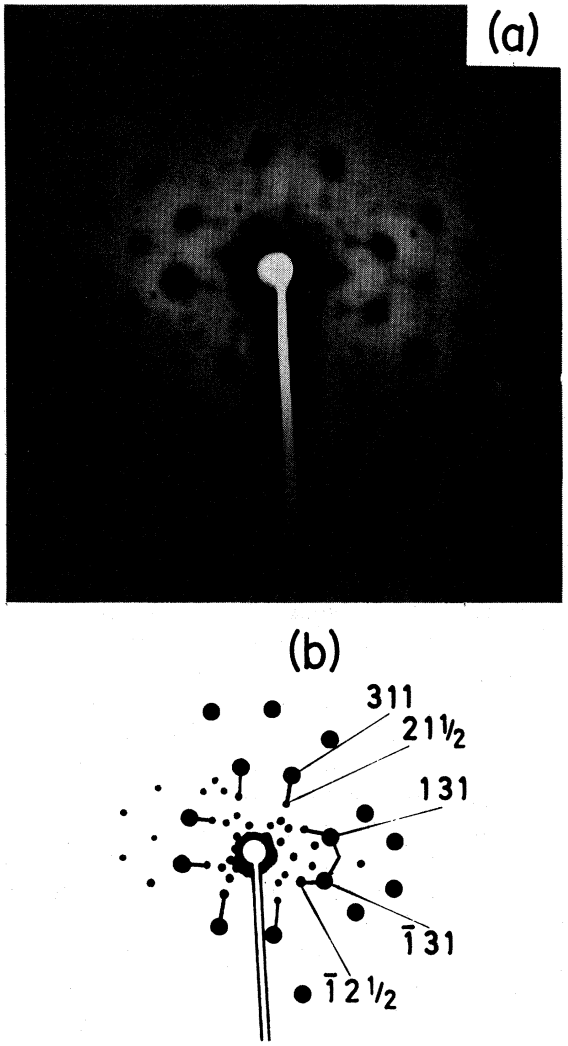


FIG. 1. (a) Diffraction pattern of Au—14.4 at. % Fe single crystal on a cylindrical photographic plate. The radiation used is monochromatic Mo$K\alpha$. The crystal is kept in a fixed orientation with the x-ray incident beam along the [001] axis. (b) Indexation of Bragg spots (●) and diffuse spots (•) seen in (a). One can notice in (a) and (b) diffuse steaks linking Bragg spots and diffuse spots [for example, (3,1,1) and (2,1,$\frac{1}{2}$).]

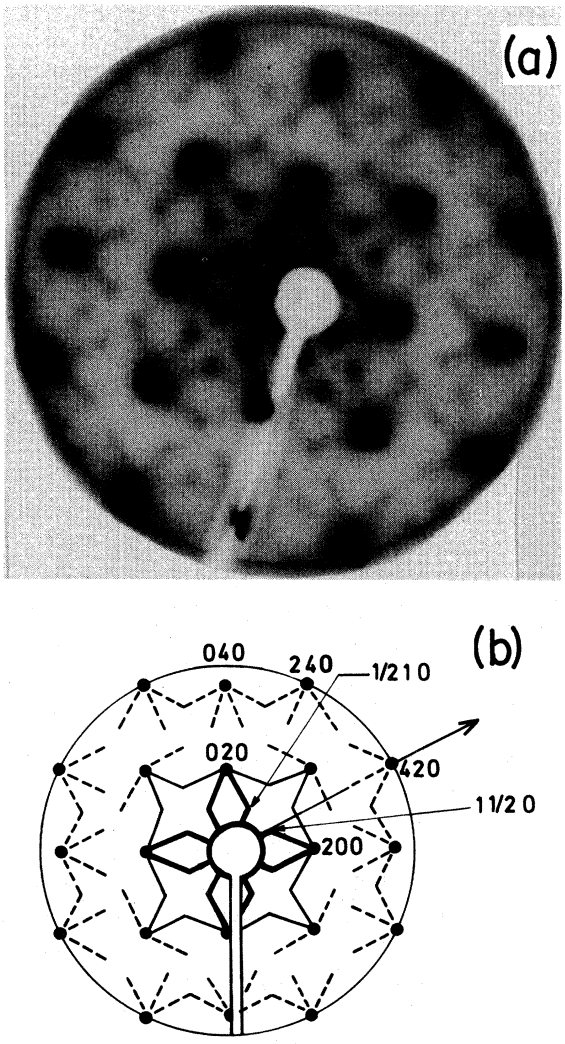


FIG. 2. (a) Diffraction pattern of Au—19 at. % Fe single crystal. The radiation used is monochromatic Ag$K\alpha$, the second harmonic is slightly visible for (2,0,0) and (2,2,0) spots. The Buerger precession apparatus is set up for the ($hko$) reciprocal plane. (b) Indexation of Bragg spots and diffuse streaks. The [420]* reciprocal axis is represented by an arrow. We have sketched the effect of modulation of the intensity along a diffuse streak superimposed on the symmetry in intensity on each side of a Bragg spot.

ferent orientations of fixed crystals, together with the precession photograph of the ($hko$) reciprocal plane for all three concentrations (Fig. 2) allow a description of the reciprocal space (Fig. 3) Each Bragg spot is starred with 12 axes [1 $\bar{\frac{1}{2}}$ 0]* (and equivalents in the cubic system) which correspond in direct space to the 12 [420] planes of different orientations. Within this elementary description the increase of intensity near (1,$\frac{1}{2}$,0) spots is simply explained by the intersection of four diffuse streaks which are connected to four different Bragg spots, as shown in Fig. 3. As in the fixed crystal photograph of Fig. 1, the precession photograph (Fig. 2) shows that the diffuse streaks do not extend continusously in reciprocal space, but their

intensity is strongly modulated as sketched in Fig. 2(b). For example, along an axis $[1\ \frac{1}{2}\ 0]^*$ which links the (0,0,0) and (4,2,0) Bragg spots, the diffuse streak is not observable in the $1<h<3$ region of reciprocal space.

By analogy with the *Ag*Mn alloys we should also note that no diffuse intensity is observed at (1,0,0) or equivalent forbidden points of the fcc reciprocal lattice. Finally one observes that the intensity of the diffuse streak along an axis $[1\ \frac{1}{2}\ 0]^*$ does not appear symetrically spread on each side about a Bragg spot crossed by the axis; it is only visible towards the smaller angle direction of the axis. For example, around the (200) reflection, only that part of the streaks extending towards small angles is visible on the precession photograph (Fig. 2). This intrinsic asymmetry must not be confused with the general tendency of the diffuse intensity to decrease towards large angles, as indeed, diffuse streaks are again observed at larger angles [up to (4,2,0) Bragg spots] on the same photograph.

### B. A simple model for local order in *Au*Fe

In the following we attempt a description of the short-range order in the *Au*Fe alloys consistent with our series of observations. We first note that the presence of diffuse small-angle scattering immediately suggest possible segregation effects in the alloy, contrary to what we observe in the *Ag*Mn alloys[21] to be discussed below. Indeed, in this way the 12 $\langle 1\ \frac{1}{2}\ 0\rangle^*$ axes supporting the diffuse streak indicate in real space the existence of platelets with a concentration different from that of the matrix and oriented along the 12 $\{420\}$ and equivalent orientations. We account for the asymetry of the streak intensity along its axis through a Bragg spot by a distortion effect.

Indeed, if the atoms of the platelets are smaller and have a scattering factor smaller than that of the matrix, such an asymmetry favoring the scattering towards smaller angles is expected.[25] This suggests that the $\{420\}$ platelets consist predominently of Fe atoms which are smaller in size than the Au atom and have a smaller scattering factor. As the half-width of the streaks is about $a^*/8$ (where $a^*=a^{-1}$ is the inverse parameter of the fcc cell) we infer that the correlation length of a platelet parallel to its (420) plane is no greater than eight fcc cells, i.e., 30 Å. In this picture the strong intensity modulation present along the streak is directly related to the structure factor of the platelet giving rise to the streak, i.e., the number of (420) planes within it. A one-plane thick platelet will give rise to a continuous diffuse streak in reciprocal space, whereas if the platelet is several planes thick these are expected to scatter coherently and thus modulate, according to their structure factor, the diffuse streak intensity. In particular, a two-plane thick platelet will give rise to a diffuse scattering in qualitative agreement with what we observe. Indeed it is possible to calculate the amplitude scattered by a crystal containing $\nu$ segregated platelets. We suppose that every platelet is made of two (420) planes, with a size of $N_1(a\sqrt{5}/2)$ in the $[\bar{1}\,2\,0]$ direction and $N_2(a/2)$ in the [001] direction (as in Fig. 4), where $a$ is the parameter of the fcc cell. The scattered amplitude $A$ is the sum of the amplitude given by an homogeneous crystal of the same volume plus the amplitude given by the platelets alone, subtracting, of course, the contribution from that part of the homogeneous crystal substituted for the platelets. Assuming that all the segregated platelets have the same size $(N_1,N_2)$, the scattered intensity $I=AA^*$ is calculated. The contribution to diffuse scattering which results is (in electron units):

$$I_{420}=4\nu\Delta f^2\cos^2\pi\left[\frac{h-k}{2}\right]\frac{\sin^2N_1\pi(h/2-k)}{\sin^2\pi(h/2-k)}\frac{\sin^2N_2\pi l}{\sin^2\pi l}\quad (l\text{ even}) \tag{1}$$

and

$$I_{420}=4\nu\Delta f^2\cos^2\pi\left[\frac{h-k}{2}\right]\frac{\sin^2N_1\pi(h/2-k+\frac{1}{2})}{\sin^2\pi(h/2-k+\frac{1}{2})}\frac{\sin^2N_2\pi l}{\sin^2\pi l}\quad (l\text{ odd})\,, \tag{2}$$

where $\Delta f$ is the difference between the mean atomic scattering factor of the atom inside the platelet, and in the matrix $(h,k,l)$ are the components of the vectors of the reciprocal lattice.

For a crystal containing 12 kinds of $\{420\}$ platelets with distinct orientations, the diffuse scattered intensity is the sum of all of them. Along an axis, the intensity is modulated by the factor

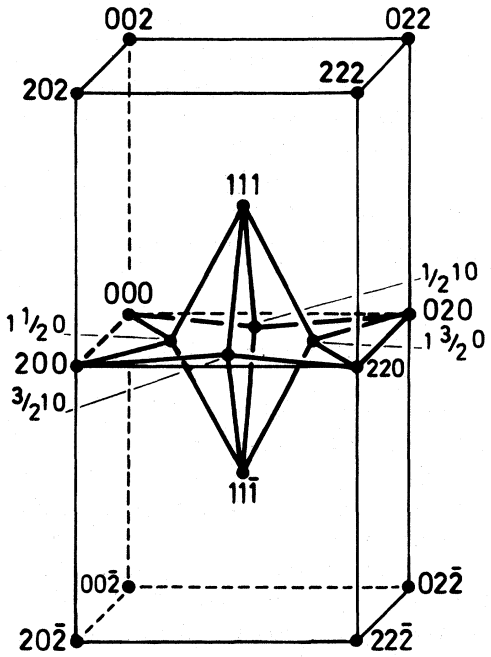


FIG. 3. Schematic representation of the reciprocal space for *Au*Fe alloy crystals, showing the intersection of four diffuse streaks around a $(1,\frac{1}{2},0)$ spot. The 24 diffuse streaks around a Bragg spot are not all represented for clarity.

$\cos^2\pi[(h-k)/2]$, due to the interference between the two (420) planes of the platelet. Figure 5 gives the experimental variation of intensity along a $[1\,\frac{1}{2}\,0]^*$ axis, compared with what is expected within such a model. One obtains a qualitative agreement between experiment and theory for the overall variation of intenisty for $0.1 < k < 2$ reciprocal-lattice units. However, the peaks indexed, $(1,\frac{1}{2},0)$, $(a_1,a_2)$, and $(3,\frac{3}{2},0)$, reveal the crossing of the $[1\,\frac{1}{2}\,0]^*$ axis by the other equivalent axes which have not explicitly been taken into account in our simple calculation. In this calculation the platelets were supposed to be made of Fe atoms only, without distortion. Unfortunately it is not possible to determine the concentration of Fe atoms inside the platelets with photographic techniques. However, it is possible to obtain a rough estimate of the proportion of Fe atoms which are segregated in this way, by comparing the intensity scattered by a diffuse streak near a (2,0,0) spot and the integrated intensity of the (2,0,0) Bragg spot.

The intensity of a diffuse streak near (2,0,0) integrated perpendicularly to the $[1,\frac{1}{2},0]$ direction, normalized to the integrated (2,0,0) intensity, is

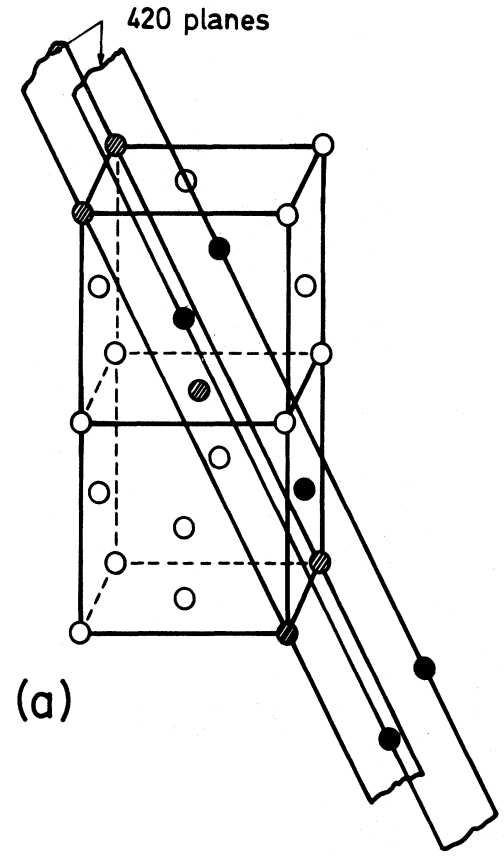


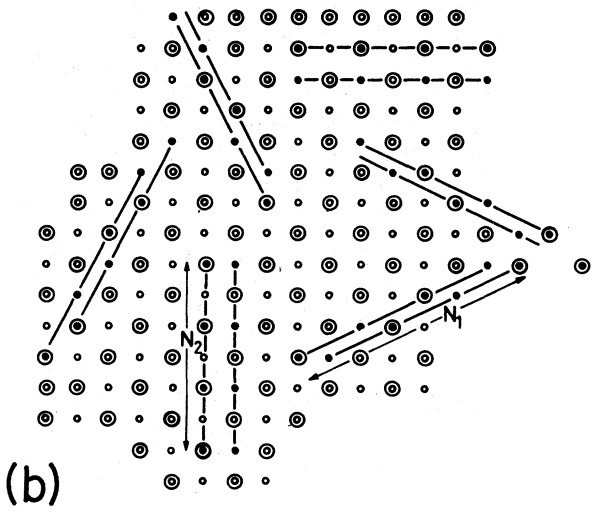


FIG. 4. (a) Representation of the model proposed for local order in *Au*Fe alloy crystals: ◍ Fe atoms in one (420) plane and ● Fe atoms in the adjacent (420) plane. (b) Intersection of the differently oriented (420) platelets with two adjacent (100) planes: ○ Au atoms at 0 level, ◎ Au atoms at $\frac{1}{2}$ level, • Fe atoms at 0 level, ⊙ Fe atoms at $\frac{1}{2}$ level. $N_1$ and $N_2$ give the size of the platelets in two different directions.

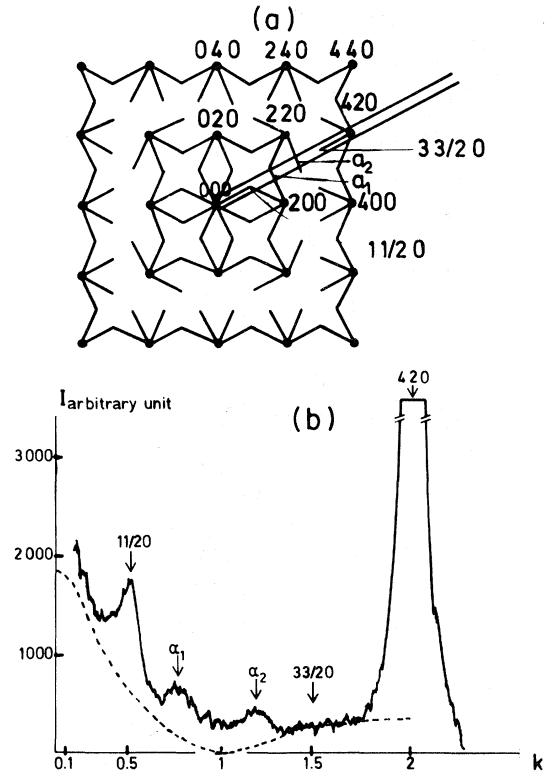


FIG. 5. (a) Representation of a $(hko)$ plane. The double line indicates the [420]* direction along which the microdensitometric measurements of (b) were performed. (b) Recording of the scattered intensity along a (420) axis, performed on the precession photograph of Fig. 2. The continuous line represents experimental results showing the extra peaks that arise from the intersection with other axes, as it is schematized in (a) and explained in the text. The dotted line represents a variation of Eq. (3): $(1-c)^2\ (f_{\mathrm{Au}}-F_{\mathrm{Fe}})^2\cos^2(\pi/2)(h-k)$.

$$I(h,k,l)=\frac{4\nu(1-c)^2(f_{\mathrm{Au}}-f_{\mathrm{Fe}})^2\cos^2\pi[(h-k)/2]}{N[(1-c)f_{\mathrm{Au}}+cf_{\mathrm{Fe}}]^2}\ , \tag{3}$$

where $N$ is the number of fcc cells of the crystal. No important corrections are made if $I(h,k,l)$ is measured near the Bragg spot. If all Fe atoms are segregated in platelets, the concentration $\nu/N$ of platelets is (for one kind of orientation)

$$\frac{c}{12\times N_1\times N_2\times 2}=\frac{\nu}{N}\ , \tag{4}$$

where $c$ is the atomic concentration of Fe atoms in the alloy. In the case of the 19% alloy, from microdensitometer measurement of the width of the streaks we measure $N_2=16$, $N_1=(8\times 2)/\sqrt{5}\simeq 8$, yielding $\nu/N=6.2\times 10^{-5}$ by (4). From these results and Eq. (3) we evaluate the intensity of a diffuse streak to be $10^{-4}$ times the intensity of a Bragg spot at the (2,0,0) reflection which is of the same order of magnitude as our microdensitometer estimate. It was not possible to perform quantitative x-ray small-angle scattering experiments in order to measure more precisely this ratio, because of the strong absorption and fluorescence of the sample.

## IV. DISCUSSION

The aim of this paper was primarily to investigate, by x-ray-diffuse scattering, the nature of the atomic short-range order present in *Au*Fe alloys. Such a study was necessary as the interpretation of a large body of magnetic data has repeatedly relied on the existence of such phenomena. Indeed the extreme sensitivity of the magnetization of these alloys on thermal history has always been associated with changes in the local arrangment of Fe atoms.[10] One of our main hopes was not only to determine the short-range order present on an atomic scale but also to try to understand how changes in magnetic properties (and spin-glass properties) are correlated with changes in the short-range order. To be fair, only the first part of this program has been achieved in this paper.

We have found evidence of very similar short-range order for the three concentrations studied here (14.4, 15.4, and 19 at. % Fe), although the first and the last alloy belong, respectively, to the spin-glass and the ferromagnetic region of the phase diagram. This would indicate that the percolation threshold for ferromagnetism occuring at 15% Fe is not due to the onset of atomic ordering in the alloy. We have interpreted the diffuse scattering as being generated by two-plane thick, 30-Å wide, Fe-rich platelets parallel to (420) planes and equivalent planes in the fcc system. As our initial study was made on bulk single crystals which were quenched from about the melting point, we have looked for qualitative changes in the diffuse scattering patterns after typical heat treatments known to strongly affect the magnetization, such as a longtime anneal at moderate temperature (150 °C) or quenching from a temperature below the melting point (650 °C). No qualitative changes occured in the diffuse scattering. This negative result shows that we are probably missing some atomic reorganization of the alloy on a much larger scale than that investigated, and that only quantitative measurement of the diffuse scattering

and Bragg scattering will enable one to resolve this apparent paradox.

Nevertheless, our findings allow us to speculate on the possible magnetic structure of the Fe-rich platelets. By inspection of Fig. 4(a), where the Fe atoms are sketched in black and hatched circles on each (420) plane, one readily sees that within each plane the Fe atoms are second (and third) neighbors but that each Fe atom in one plane is a nearest neighbor of three Fe atoms in the other plane. Assuming a ferromagnetic interaction take place between two nearest-neighbor Fe atoms ensures that the whole assembly will be ferromagnetic and because of the shape anisotropy of the two plane configurations, the resultant magnetic moment will lie in the (420) plane. This conjecture will not be easy to check as there are 12 inequivalent directions to start with. Finally, one should consider whether our model for the segregation of Fe has a direct impact on transport properties, particularly on the resistivity. From the work of Sundahl[26] it appears that the resistivity of Fe in Au is linear in Fe concentration only below 5% Fe. Above this value the resistivity is less than expected from a linear extrapolation and this deviation is dramatically increased by going to low temperatures (4.2 K as compared to 300 K) showing unambiguously the onset of magnetic ordering superimposed onto the short-range-order effect present at all temperatures. We may conclude from our work that the fact that the low-temperature resistivity becomes very sensitive to the thermal history (in the range 10–20 % Fe) reflects the magnetic percolation between the Fe-rich platelets rather than the segregation of individual Fe atoms.

In conclusion, the essentially different nature of short-range order existing in *Ag*Mn (and most certainly *Cu*Mn as well) and *Au*Fe should be emphasized.

While in the former system we have determined[27] that no important scattered intensity is observed at small angles (which means that only homogeneous models for short-range order must be considered), the *Au*Fe system unambiguously shows a tendency towards segregation of Fe-rich microdomains which we have described by our platelet model.

## ACKNOWLEDGEMENTS

We are indebted to the Service de Diffusion et de Technologie des Matériaux (SDTM) CNRS at Orsay for the preparation of the *Au*Fe and *Ag*Mn alloy single crystals. We thank Dr. Bizouard and F. Charpentier for the microprobe analysis of these alloys. We especially thank Dr. Caudron and Dr. Costa (Service O.M. ONERA-Chatillon) for providing us with the starting *Au*Fe alloys necessary for this work.

[1]J. Owen, M. E. Browne, V. Arp, and A. F. Kip, J. Phys. Chem. Solids 2, 85 (1957).

[2]V. Cannella and J. A. Mydosh, Phys. Rev. B 6, 4 220 (1972).

[3]P. W. Anderson, *Ill Condensed Matter,* Proceeding of the Les Houches Summer School, Session 3, 1978, edited by R. Balian *et al.* (North-Holland, New York, 1979), Chap. 3.

[4]S. F. Edwards and P. W. Anderson, J. Phys. F 5, 965 (1975); D. Sherrington and S. Kirkpatrick, Phys. Rev. Lett. 35, 1792 (1975).

[5]J. Souletie and R. Tournier, J. Low Temp. Phys. 1, 95 (1969).

[6]A. Blandin, J. Phys. (Paris) Colloq. 39, C6-1499 (1978), and references therein.

[7]J. L. Tholence and R. Tournier, Physica 86–88B, 873 (1977).

[8]P. A. Beck, Prog. Mater. Sci. 23, 1 (1978).

[9]R. W. Tustison and P. A. Beck, Solid State Commun. 19, 1075 (1976)

[10]S. Crane and H. Claus, Solid State Commun. 35, 461 (1980); Phys. Rev. Lett. 46, 1693 (1981).

[11]B. R. Coles, B. V. B. Sarkissian, and R. H. Taylor, Philos. Mag. B 37, 489 (1978).

[12]A. P. Murani, J. Phys. F 4, 757 (1974); S. Nagata, P. H. Keesom, and H. R. Harrison, Phys. Rev. B 19, 1633 (1979).

[13]E. Scheil and E. Wachtel, Z. Metallkd. 49, 590 (1958).

[14]D. P. Morris and I. Williams, Proc. Phys. Soc. London 73, 422 (1959).

[15]J. J. Smit, G. J. Nieuwenhuis, and L. J. de Jongh, Solid State Commun. 31, 265 (1979); 32, 233 (1979).

[16]G. L. Whittle, R. Cywinski, and P. E. Clark, J. Phys. F 10, L311 (1980).

[17]A. P. Murani, S. Roth, P. Radhakrishna, B. D. Rainford, B. R. Coles, K. Ibel, G. Goeltz, and F. Mezei, J. Phys. F 6, 425 (1976).

[18]T. M. Hayes, J. W. Allen, J. B. Boyce, and J. J. Hauser, Phys. Rev. B 22, 4503, (1980).

[19]H. Sato, S. A. Werner, and R. Kikuchi, J. Phys. 35,

23 (1974); H. Sato, S. A. Werner, and M. Yessik, in *Magnetism and Magnetic Materials—1971 (Chicago),* Proceedings of the 17th Annual Conference on Magnetism and Magnetic Materials, edited by O. C. Graham and J. J. Ryne (AIP, New York, 1971), p. 509; in *Magnetism and Magnetic Materials—1972 (Denver),* Proceedings of the 18th Annual Conference on Magnetism and Magnetic Materials, edited by C. D. Graham and J. J. Rhyne (AIP, New York, 1973), p. 679; S. A. Werner and J. W. Cable, J. Appl. Phys. 52, 1757 (1981).

[20]D. Meneghetti and S. S. Sidu, Phys. Rev. 105, 130 (1957).

[21]H. Bouchiat, E. Dartyge, P. Monod, and M. Lambert, Phys. Rev. B 23, 1375 (1981).

[22]H. Bizouard and F. Charpentier (private communication).

[23]J. Godard and J. P. Chapelle, Service de Diffusion et de Technologie des Matériaux (S.D.T.M.) CNRS-ORSAY.

[24]M. J. Buerger, *X-ray Crystallography* (Wiley, New York, 1958).

[25]A. Guinier, *Théorie et Technique de la Radiocristallographie* (Donod, Paris 1956), p. 600.

[26]R. C. Sundahl, T. Chen, J. M. Sivertsen, and Y. Sato, J. Appl. Phys. 37, 1024 (1966).

[27]H. Bouchiat (unpublished).

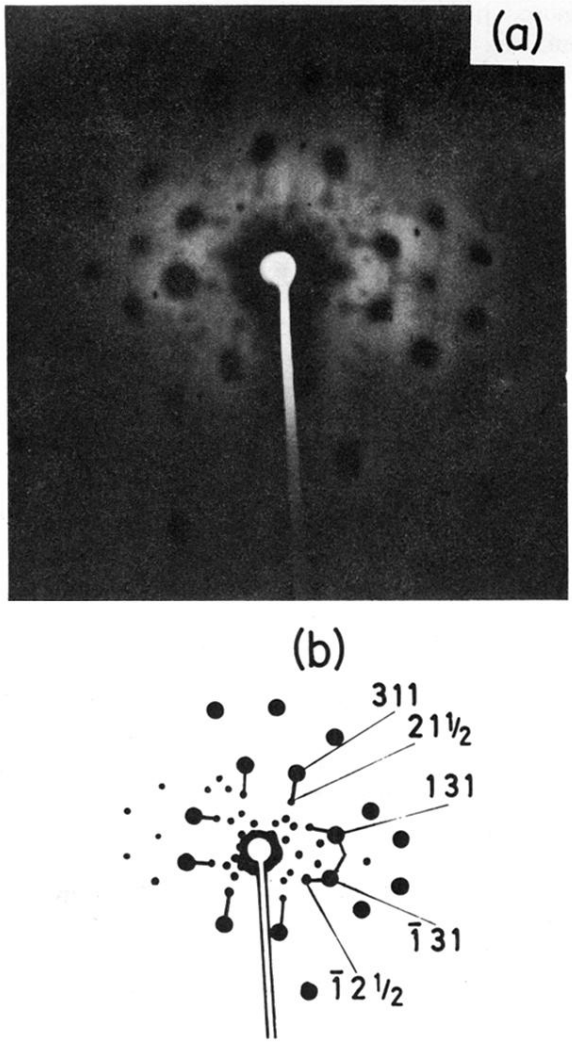


FIG. 1. (a) Diffraction pattern of Au—14.4 at. % Fe single crystal on a cylindrical photographic plate. The radiation used is monochromatic Mo $K\alpha$. The crystal is kept in a fixed orientation with the x-ray incident beam along the [001] axis. (b) Indexation of Bragg spots (●) and diffuse spots (•) seen in (a). One can notice in (a) and (b) diffuse steaks linking Bragg spots and diffuse spots [for example, (3,1,1) and $(2,1,\frac{1}{2})$.]

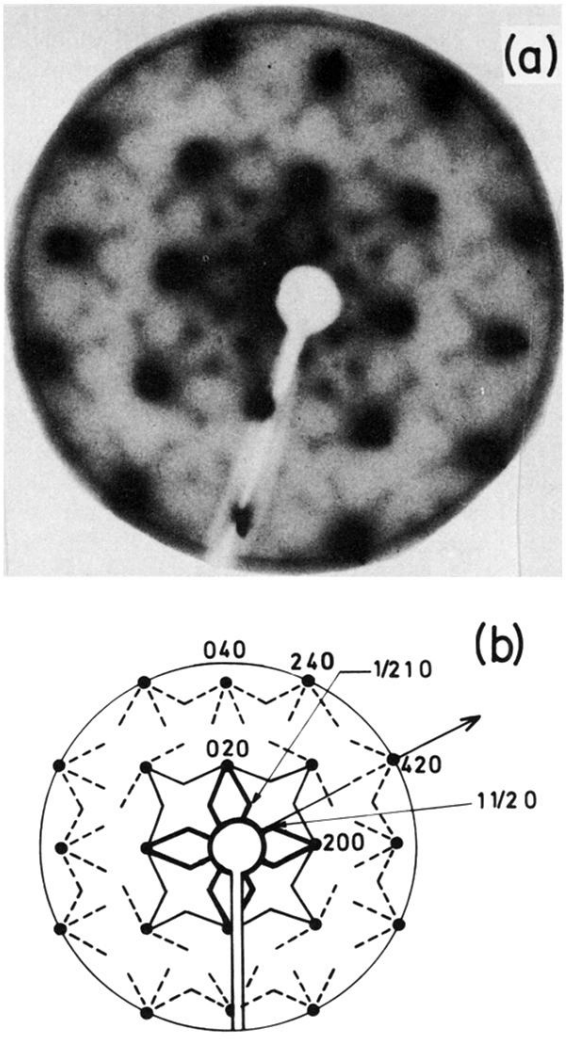


FIG. 2. (a) Diffraction pattern of Au – 19 at. % Fe single crystal. The radiation used is monochromatic Ag $K\alpha$, the second harmonic is slightly visible for (2,0,0) and (2,2,0) spots. The Buerger precession apparatus is set up for the ($hko$) reciprocal plane. (b) Indexation of Bragg spots and diffuse streaks. The [420]* reciprocal axis is represented by an arrow. We have sketched the effect of modulation of the intensity along a diffuse streak superimposed on the symmetry in intensity on each side of a Bragg spot.